

Surface Analysis by Highly Charged Ion Based Secondary Ion Mass Spectrometry

T. Schenkel,¹ A. V. Hamza,¹ A. V. Barnes,¹ M. W. Newman,¹ G. Machicoane,¹ T. Niedermayer,¹ M. Hattass,¹ J. W. McDonald,¹ D. H. Schneider,¹ K. J. Wu² and R. W. Odom²

¹Lawrence Livermore National Laboratory, Livermore, California, USA;

²Charles Evans & Associates, Redwood City, California, USA

Received September 14, 1998; revised October 23, 1998; accepted November 15, 1998

PACS ref: 82.80.Ms, 07.75+h

Abstract

Electronic sputtering in the interaction of slow ($v < 10^6$ m/s), highly charged ions (e.g., Au^{69+}) with solid surfaces increases secondary ion yields by over two orders of magnitude compared to sputtering with singly charged ions. We discuss advantages of highly charged ions for analysis of semiconductors and biomolecular solids in a time-of-flight secondary ion mass spectrometry scheme.

1. Introduction

The availability of surface analysis techniques with high sensitivity and sub-micron spatial resolution is critical for advancement in integrated circuit fabrication [1]. Time-of-flight secondary ion mass spectrometry (TOF-SIMS) has been developed into a versatile tool for analysis of impurities on silicon wafers [2,3]. Typical sensitivities for metal impurities are $\sim 10^9$ atoms/cm². Focusing of the primary beam enables particle identification with spatial resolutions of a few hundred nanometers [3]. Analysis of solid biomaterials is another important application field of TOF-SIMS. Here, problems requiring structural identification at the molecular level can be addressed [4].

Development of Electron Beam Ion Traps (EBIT) at Lawrence Livermore National Laboratory has made beams of slow ($1 \text{ keV} < E_{\text{kin}} < 1 \text{ MeV}$), very highly charged ions, like Au^{69+} , available for ion solid interaction studies [5]. Strong electronic sputtering was found to produce secondary ion yield increases by several orders of magnitude compared to sputtering by singly charged ions [6]. Measurements of total ablation rates showed that ionization probabilities for secondary particles increased by an order of magnitude as a function of projectile charge to a value of $\sim 8\%$ for Th^{70+} , in sputtering of heavy metal oxides [7,8].

2. Experimental

A schematic of the experimental setup is shown in Fig. 1. Highly charged ions (HCI) are extracted from EBIT and reach the target chamber after momentum analysis in a 900 bending magnet. TOF-SIMS is practical with a flux of only ~ 100 up to more than 30000 HCI per second. The base pressure in the target chamber can be prepared for experiments requiring ultra high (10^{-10} torr) or just high vacuum (10^{-8} torr). In positive polarity, HCI can be decelerated to an impact energy of ~ 1 keV simply by raising the target bias close to source potential. Charged secondary particles are accelerated by the target bias and detected in the annular microchannel plate

detector, or in one of the two detectors in the reflectron. Secondary ion hits are then registered by a multi-stop timing analyzer. Depending on the polarity of the target bias, time-of-flight cycles are started by electrons or protons emitted from targets during interaction with a singly HCI. Start efficiencies are 100% for electrons and copious proton emission [9] gives start efficiencies of $> 50\%$ in positive polarity. An annular microchannel plate detector is used for studies where a mass resolution, $m/\Delta m$, of only ~ 50 at $m = 28$ u is sufficient but a higher transmission (0.1–0.15) is desirable. The mass resolution of the reflectron is ~ 1000 at $m = 28$ u. Spectra are built either in “histogram mode”, by adding signals from consecutive impacts, or in “list mode” where TOF-cycles from individual impact events are stored separately. Storing data in “list mode” enables analysis of coincidences of secondary ions that were emitted in the same impact event. This technique was introduced by Schweikert *et al.* [10] who used fission fragments from ^{252}Cf to eject high yields of secondary ions from insulating samples. High secondary ion yields are a necessary condition for coincidence counting to be practical.

3. Results

In Fig. 2, we show a section of a TOF-SIMS spectrum of positive secondary ions from a SiO_2 target (150 nm thermal oxide

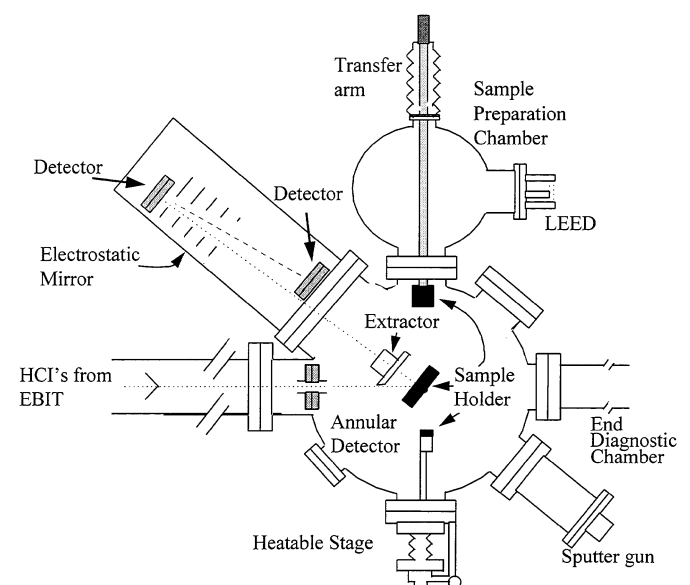


Fig. 1. Schematic of setup for HCI-SIMS.

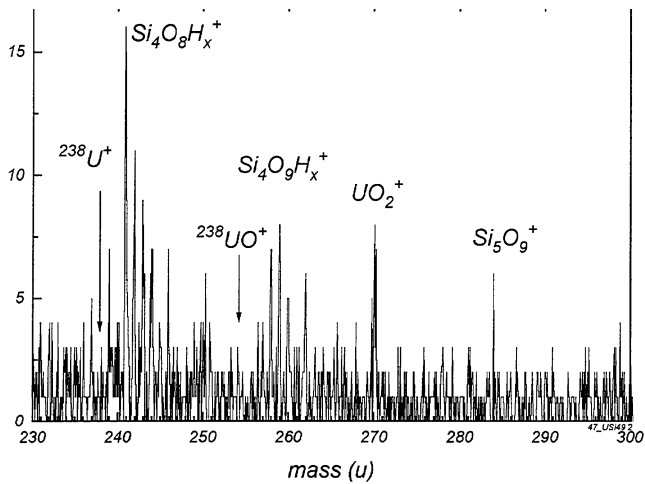


Fig. 2. HCI-SIMS spectrum of UO_2 impurities on a SiO_2 target. The spectrum was recorded in reflectron mode.

on Si). Full spectra and the increase of secondary ion yields as a function of projectile charge have been described previously [6]. Secondary ions were detected in the reflectron after passing through the electrostatic mirror. Projectiles were Xe^{44+} ($E_{\text{kin}} = 255$ keV). The target had been used as a catcher in a total sputter yield measurement and was covered with 1.4×10^{11} uranium atoms/cm² [7]. This coverage had been determined quantitatively by heavy ion backscattering [11]. Positive atomic ions (C^+ , O^+ , Si^+) dominate the spectrum from the SiO_2 substrate, indicating a high degree of dissociation in electronic sputtering [6]. For uranium oxide targets, the dominant peaks are UO^+ and UO_2^+ , followed by U^+ [7]. Uranium is very reactive and can be expected to be in an oxidized state on the SiO_2 surface. The dominant uranium signature is the UO_2^+ ion; some UH^+ is present while U^+ and UO^+ are not detected at the present background level. The ratio of detected uranium oxide ions and secondary ions from the substrate is $(2.3 \pm 0.4) \times 10^{-4}$. At a monolayer coverage of 10^{15} atoms/cm² this corresponds to an uranium coverage of 2.3×10^{11} atoms/cm²; a value which is within a factor of two of the calibrated coverage value. While the concept of Coulomb explosion is useful to understand sputtering of uranium oxide by ions like Au^{63+} and Th^{70+} [7], the data base for SiO_2 does not yet allow a conclusive differentiation of contributing mechanisms (such as defect mediated sputtering [12], effects of intense electronic excitation [8], and Coulomb explosions).

Using this calibrated target, we estimate the sensitivity of HCI based TOF-SIMS (HCI-SIMS) for detection of heavy metals on oxidized silicon surfaces to be 10^{10} atoms/cm². Studies of useful yields (i.e. secondary ion yields and total sputtering yields) for HCI induced particle emission from silicon wafers (bare and oxidized) are in progress.

In Fig. 3, we demonstrate the coincidence counting technique in HCI-SIMS. The target was a test wafer of thermally grown SiO_2 on Si with a tungsten pattern. Tungsten was deposited by reaction of WF_6 with Si_2H_6 at 150°C . Feature sizes were in the micrometer range. Secondary ions emitted from the target include molecular ions from tungsten and silicon dioxide areas. We recorded TOF cycles in "list-mode" and add cycles only when specific ions are present. Resulting spectra reveal correlations of secondary ions. Requiring the presence of a molecular ion characteristic for the silicon

dioxide areas, i.e. SiO^+ , gives a spectrum where specific peaks are suppressed. Requiring the presence of a tungsten feature (WO^+) shows silicon fluoride ions in coincidence. Emission of WO^+ and Si_xF^+ ions is highly correlated. Virtually no Si_xF^+ ions are emitted when SiO^+ is present, i. e., when the projectile probed the silicon dioxide areas of the target. Coincidence counting shows that the Si_xF^+ impurities are localized on the regions patterned with tungsten. They can be attributed to be byproducts of the WF_6 reduction step.

In this example, the feature size was rather large and other techniques such as Auger electron microscopy or conventional TOF-SIMS could have determined the location of Si_xF_y impurities easily. The area of secondary ion emission in individual HCI impact events has an estimated diameter of ~ 10 nm [10], allowing characterization of particles and feature sizes beyond currently available resolution limits [3]. Analyzing many nanometer sized features simultaneously removes constraints due to the small number of impurities in one region. A further advancement will lie in combining secondary ion detection with imaging in an emission microscope scheme [13].

Figure 4 shows an example of the analysis of a biomolecular solid by HCI-SIMS (Xe^{44+} , $E_{\text{kin}} = 20$ keV). We have studied

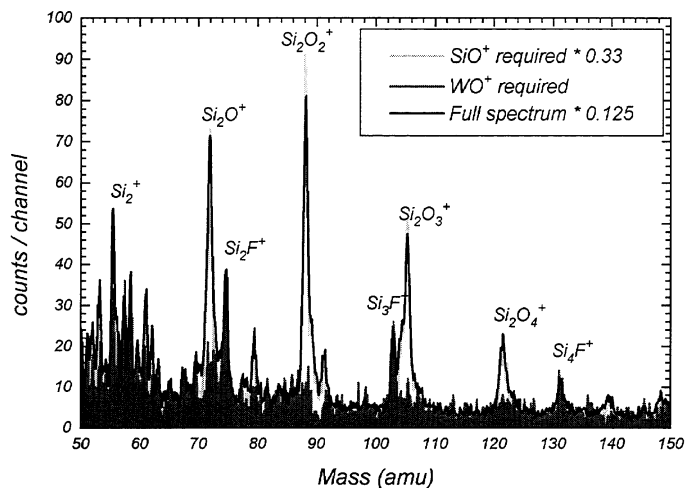


Fig. 3. Coincidence counting of positive secondary ions from a W/SiO_2 wafer.

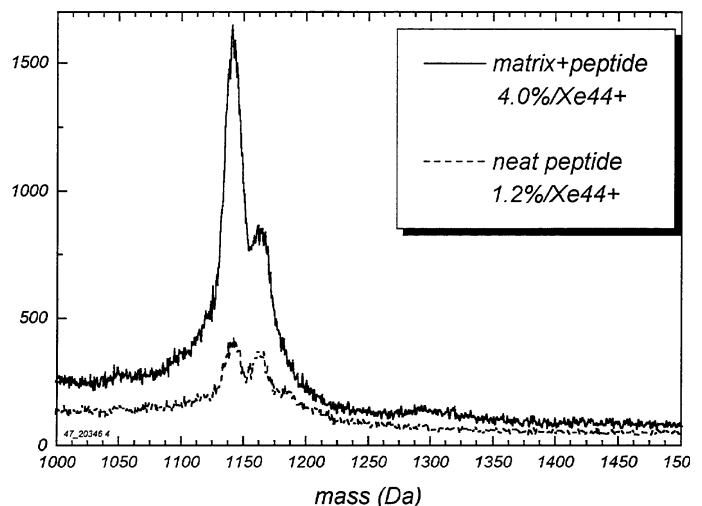


Fig. 4. Positive secondary ions from neat gramicidin S and gramicidin S mixed with 2,5-dihydroxybenzoic acid.

gramicidin S samples comparing secondary ion emission from neat samples and samples where the peptide had been embedded in a standard matrix, 2,5-dihydroxybenzoic acid. The yield (detected ions per projectile) for intact gramicidin S from the matrix containing sample was 0.04 per Xe^{44+} , about three times higher than for the neat peptide sample. The concentration ratios of matrix and analyte molecules was $\sim 5000:1$. Embedding of analyte molecules in matrix solutions is known to produce strongly enhanced yields of intact biomolecular ions both for laser and singly charged ion induced ablation [14]. Mechanisms yielding this enhancement are not well understood.

Applying the coincidence technique, we investigated the interaction of matrix and analyte molecules. At the given concentration of analyte molecules in the matrix, each HCI produces secondary ions from a volume containing at average less than one analyte molecule. Preliminary results indicate a strong correlation in the emission of molecular ions from analyte and matrix. This observation points towards pre-formed ions in the solid state as responsible for the matrix enhancement effect. Ion formation through collisional charge exchange in the gas phase seems unlikely, since the density of desorbed molecules is too low.

5. Conclusion

Research in surface analysis has created an array of very potent techniques. In mass spectrometry, use of singly charged ions, neutral atoms, fast (>1 MeV/u) heavy ions and lasers is well established. More recently, advantages of charged cluster beams have been investigated [4]. The examples given in this article demonstrate capabilities of

highly charged ions like Xe^{44+} and Au^{69+} for sensitive ($\leq 10^{10}$ atoms/cm²) surface analysis with very high spatial resolution ($\ll 100$ nm). Determination of physical limits for detection sensitivity and spatial resolution is object of ongoing research. The latter will determine which applications will be served best by HCI-SIMS.

Acknowledgement

This work was performed under the auspices of the U. S. Department of Energy by Lawrence Livermore National Laboratory under contract No. W-7405-ENG-48.

References

1. The National Technology Roadmap for Semiconductors (Semiconductor Industries Association, San Jose, Ca, 1994).
2. Schnieders, A. *et al.*, J. Vac. Sci. Technol. B **14**, 2712 (1996).
3. Diebold, A. C. *et al.*, J. Vac. Sci. Technol. B **16**, 1825 (1998).
4. For a recent overview see: *Secondary Ion Mass Spectrometry-SIMS XI*, (G. Gillen, R. Lareau, J. Bennett and F. Stevie (eds.) (Wiley, Chichester, 1998).
5. Schneider, D. H. and Briere, M. A. Physical Scripta. **53**, 228 (1996), and references therein.
6. Schenkel, T. *et al.*, Nucl. Instrum. Meth. Phys. Res. B **125**, 153 (1997); Schenkel, T. *et al.*, J. Vac. Sci. Technol. A **16**, 1384 (1998).
7. Schenkel, T. *et al.*, Phys. Rev. Lett. **80**, 4325 (1998).
8. Schenkel, T. *et al.*, Phys. Rev. Lett., in press.
9. Schenkel, T. *et al.*, Phys. Rev. Lett. **78**, 2481 (1997).
10. Park, M. A. Gibson, K. A. Quinones, L. and Schweikert, E. A., Science **248**, 988 (1990).
11. Banks, J. C. *et al.*, Nucl. Instrum. and Methods Phys. Res. B **136**, 1223 (1998).
12. Sporn, M. *et al.*, Phys. Rev. Lett. **79**, 945 (1997).
13. Barnes, A. V. *et al.*, to be published.
14. Wu, K. J. and Odom, R. W., Anal. Chem. **68**, 873 (1996).